

Article

The Potential of the Superhydrophobic State to Protect Magnesium Alloy against Corrosion

Kirill A. Emelyanenko ^{1,*}, Elizaveta V. Chulkova ¹, Alexey M. Semiletov ¹, Alexander G. Domantovsky ¹, Valeria V. Palacheva ², Alexandre M. Emelyanenko ¹ and Ludmila B. Boinovich ^{1,*}

¹ Surface Forces Laboratory, A.N. Frumkin Institute of Physical Chemistry and Electrochemistry, Leninsky Prospekt 31 bldg. 4, 119071 Moscow, Russia; chulkova_liza@mail.ru (E.V.C.); semal1990@mail.ru (A.M.S.); doman-alex@yandex.ru (A.G.D.); ame@phyche.ac.ru (A.M.E.)

² Department of Physical Metallurgy of Non-Ferrous Metals, National University of Science and Technology "MISIS", Leninsky Ave. 4, 119049 Moscow, Russia; palacheva@misis.ru

* Correspondence: emelyanenko.kirill@gmail.com (K.A.E.); boinovich@mail.ru (L.B.B.); Tel.: +7-495-955-4497 (K.A.E.); +7-495-955-4625 (L.B.B.)

Abstract: We describe the technologically simple route for the fabrication of the superhydrophobic coatings on top of wrought magnesium alloy MA8 based on nanosecond laser processing followed by the chemical vapor deposition of fluorosilane. The chemical and phase composition, surface morphologies, and variation of the coating wettability during prolonged contact with 0.5 NaCl solution or with salt aerosol were characterized using X-ray diffraction, FT-IR spectroscopy, scanning electron microscopy measurements, and the wettability analysis. The as-prepared coatings demonstrate corrosion current of more than eight orders of magnitude lower, while after 30 days of sample immersion into corrosive solution, the current was four orders of magnitude lower than that obtained for a polished sample which was for only 2 h in contact with electrolyte. The mechanisms of the protective activity of fabricated coatings were discussed.

Keywords: superhydrophobicity; magnesium; corrosion resistance; nanosecond laser treatment; durability; EIS; salt spray



Citation: Emelyanenko, K.A.; Chulkova, E.V.; Semiletov, A.M.; Domantovsky, A.G.; Palacheva, V.V.; Emelyanenko, A.M.; Boinovich, L.B. The Potential of the Superhydrophobic State to Protect Magnesium Alloy against Corrosion. *Coatings* **2022**, *12*, 74. <https://doi.org/10.3390/coatings12010074>

Academic Editor: Fabio Palumbo

Received: 28 December 2021

Accepted: 7 January 2022

Published: 9 January 2022

Publisher's Note: MDPI stays neutral with regard to jurisdictional claims in published maps and institutional affiliations.



Copyright: © 2022 by the authors. Licensee MDPI, Basel, Switzerland. This article is an open access article distributed under the terms and conditions of the Creative Commons Attribution (CC BY) license (<https://creativecommons.org/licenses/by/4.0/>).

1. Introduction

The increasing applications of wrought magnesium alloys in electronics, biomedical, aerospace, and defense industries with their simultaneous limited corrosion resistance in various environments cause concern in the scientific community, which has researched corrosion-protective coatings.

During recent decades the numerous approaches to cost-effectively increase the corrosion resistance of magnesium alloys based on the surface modification have been discussed in the literature [1–24]. As examples of these approaches, here we would like to mention the modification of the magnesium surface by sol-gel precoatings [5], anodization followed by different postanodization treatments [6], cold spray layers [7], various conversion coatings [5–8] including Mg-Al layered double hydroxide, hydroxide, and magnesium phosphate layers. Particular attention was paid to the application of the water-repelling coatings, such as superhydrophobic or slippery liquid-infused porous coatings, to protect the magnesium coatings against electrolytic and microbiologically induced corrosion [12–24].

Although several of the presented studies are technologically attractive and their resistance in the corrosive media looks promising, the studies, where the detailed analysis of the evolution of the surface properties in prolonged contact with aggressive liquids, remain scarce. Besides, the mechanisms of degradation of the anticorrosive properties upon continuous contact with chloride-containing solutions require further discussion.

In this study, we present the technologically simple route for preparing the superhydrophobic coating on top of wrought magnesium alloy and discuss the behavior of

the surface and electrochemical parameters of the fabricated coating during its prolonged and continuous contact with the corrosive medium. We will show a high potential of a hierarchically organized layer of magnesium oxide covered by a layer of fluorooxysilane to significantly protect the magnesium alloy surface against corrosion.

2. Materials and Methods

2.1. Sample Preparation

In this study, we prepared the superhydrophobic samples from the wrought magnesium alloy MA8 and studied the properties and the electrochemical behavior of obtained samples in corrosive solutions and the conditions of the salt spray chamber. The nominal composition of MA8 alloy (in weight %) is given in Table 1.

Table 1. The composition of magnesium alloy MA8.

Element	Cu	Al	Mn	Fe	Si	Ce	Ni	Cu	Zn	Mg
Content, wt.%	<0.05	<0.1	1.3–2.2	<0.05	<0.1	0.15–0.35	<0.007	<0.05	<0.3	Balance

To fabricate the superhydrophobic samples for studies, we used flat coupons (3 mm thick) with a size of $20 \times 80 \text{ mm}^2$. The pretreatment of the samples included grinding and polishing with a set of SiC abrasive papers, ultrasonic washing in deionized water and air-drying. For each sample, an area of $20 \times 30 \text{ mm}^2$ at one end of the sample was subjected to laser treatment to get the hierarchical roughness. Such design of the samples matches well for the measurements of the electrochemical properties of the textured part of the sample. A set of preliminary experiments allowed selecting the following parameters of laser treatment resulted in the textures with prolonged resistance to corrosive media: the laser beam waist of $40 \text{ }\mu\text{m}$, the peak fluence of 1.8 J/cm^2 , pulse duration of 4 ns, the repetition rate of 1 MHz, the linear scanning rate of 100 mm/s , and the scanning line density of 400 mm^{-1} .

Laser system Argent-M (Saint-Petersburg, Russia) with an IR ytterbium-fiber laser YLPM (IPG Photonics, wavelength of $1.064 \text{ }\mu\text{m}$, nominal power 30 W) and a RAYLASE MS10 two-axis laser beam deflection unit (Wessling, Germany) was used for laser processing the samples. The laminar upward airflow around the sample with a velocity of 16 cm/s was applied to avoid the problem of gradient texture formation due to the gradual sample heating during the texturing process [21]. To remove surface micro- and nanoparticles weakly adhered to the sample's surface, the laser-processed samples were thoroughly washed with the deionized water jet.

To get the superhydrophobic surface, two conditions should be satisfied. The surface should have the hierarchical roughness and low surface energy is required. The hierarchical roughness of the magnesium alloy surface was achieved by laser texturing, as described above. To decrease the surface energy, we used the chemical vapor deposition (CVD) of fluorosilane $\text{CF}_3(\text{CF}_2)_7\text{CH}_2\text{O}(\text{CH}_2)_3\text{Si}(\text{OCH}_3)_3$ at a temperature of $105 \text{ }^\circ\text{C}$. Prior to CVD processing, the samples were subjected to 10 min air plasma treatment using a PCE-6 plasma cleaning machine (MTI Corporation, Richmond, CA, USA) to improve the chemisorption of the hydrophobic agent to the metal surface. Such treatment resulted in the enrichment of surface hydroxyl and carboxyl groups, which served as the chemical active centers for the fluorooxysilane adsorption. For the comparison of the corrosion resistance of the fabricated superhydrophobic sample with that of the hydrophobic one, we prepared the hydrophobic sample by chemical vapor deposition of fluorooxysilane onto a polished coupon of MA8 sample without laser texturing. After chemisorption of the fluorooxysilane, both hydrophobic and superhydrophobic samples were heat-treated at $T = 150 \text{ }^\circ\text{C}$ for the crosslinking of the neighboring fluorooxysilane molecules with the formation of siloxane bonds.

2.2. Surface Characterization

The wettability of fabricated samples was characterized by the contact and roll-off angle measurements. These angles were measured using the home-made setup [25,26] for the 15 μL deionized water droplets. The data on the wettability presented below were obtained as an average for five different droplets deposited at different locations of a studied sample.

To study the surface chemical composition of the sample without its destruction, we used Fourier-transform infrared (FTIR) reflectance spectroscopy with a Smart SAGA (Specular Apertured Grazing Angle) accessory with the angle of light incidence on the studied sample of 80° . The infrared spectra were recorded at a resolution of 4 cm^{-1} in the spectral range of $650\text{--}4000\text{ cm}^{-1}$ using a Nicolet 6700 spectrometer (Thermo Scientific, Waltham, MA, USA) equipped with a mercury cadmium telluride detector cooled with liquid N_2 . All the spectra were obtained by averaging over 128 scans.

The electrochemical properties of the fabricated coatings were studied in 0.5 M aqueous solutions of NaCl using an electrochemical workstation Elins P50x + FRA-24M (Elins, Russia). The measurements were performed in a three-electrode electrochemical cell (PAR K0235, Princeton, NJ, USA) with a magnesium alloy sample used as the working electrode (apparent circular area exposed to the electrolyte was 1 cm^2), a platinum mesh as the counter electrode, and an Ag/AgCl electrode filled with saturated KCl solution as the reference electrode. A sweep rate of 1 mV/s was applied during recording the potentiodynamic polarization curves, while the electrochemical impedance spectroscopy (EIS) measurements were conducted using a 10 mV amplitude in a frequency range from 500 mHz to 100 kHz .

Additionally, we tested the corrosion resistance of our superhydrophobic samples in the salt spray chamber (Weiss SC/KWT 450, Balingen, Germany). During this type of testing, the 5 wt.% NaCl aqueous solution was cyclically sprayed onto the tested samples at $T = 35^\circ$ for a prolonged period of time. Each cycle contained 15 min of solution spraying and 45 min of exposure to a humid water vapor atmosphere with $\text{RH} > 95\%$. To catch the appearance of the corrosion damage, the samples were visually inspected.

The surface morphology of fabricated superhydrophobic samples was studied by field-emission scanning electron microscopy using an FIB-SEM Nvision 40 workstation (Zeiss, Germany) in the secondary electron detection mode. The chemical composition was defined using an X-MAX energy-dispersive detector (Oxford Instruments, Abingdon, UK) with an accelerating voltage of 10 kV .

A D8 ADVANCE X-ray Diffractometer (Bruker, Madison, WI, USA) with $\text{Cu-K}\alpha$ radiation source was used to perform XRD analyses of the crystallographic structure of the samples. The samples were scanned in 2θ range from 10 to 60 degrees with the step of 0.05 degree, and 5 s exposition time for each step.

3. Results and Discussion

3.1. The Wettability of Superhydrophobic Samples

The fabricated samples just after laser texturing demonstrated the superhydrophilic state with rapid imbibition of the water droplet, which is related to the hierarchical roughness (Figure 1a,b) of intrinsically hydrophilic magnesium alloy surface. The observed texture is formed by the aggregates of magnesium oxide nanoparticles, deposited onto the surface from the laser plume in the course of laser ablation. The as-formed magnesium oxide layer has a low density, which results in an inappropriate Pilling–Bedworth ratio of 0.81 [27,28] and porous layer structure. Thus, for a hydrophilic sample such a porous layer does not hinder access of corrosive media to the magnesium/oxide interface.

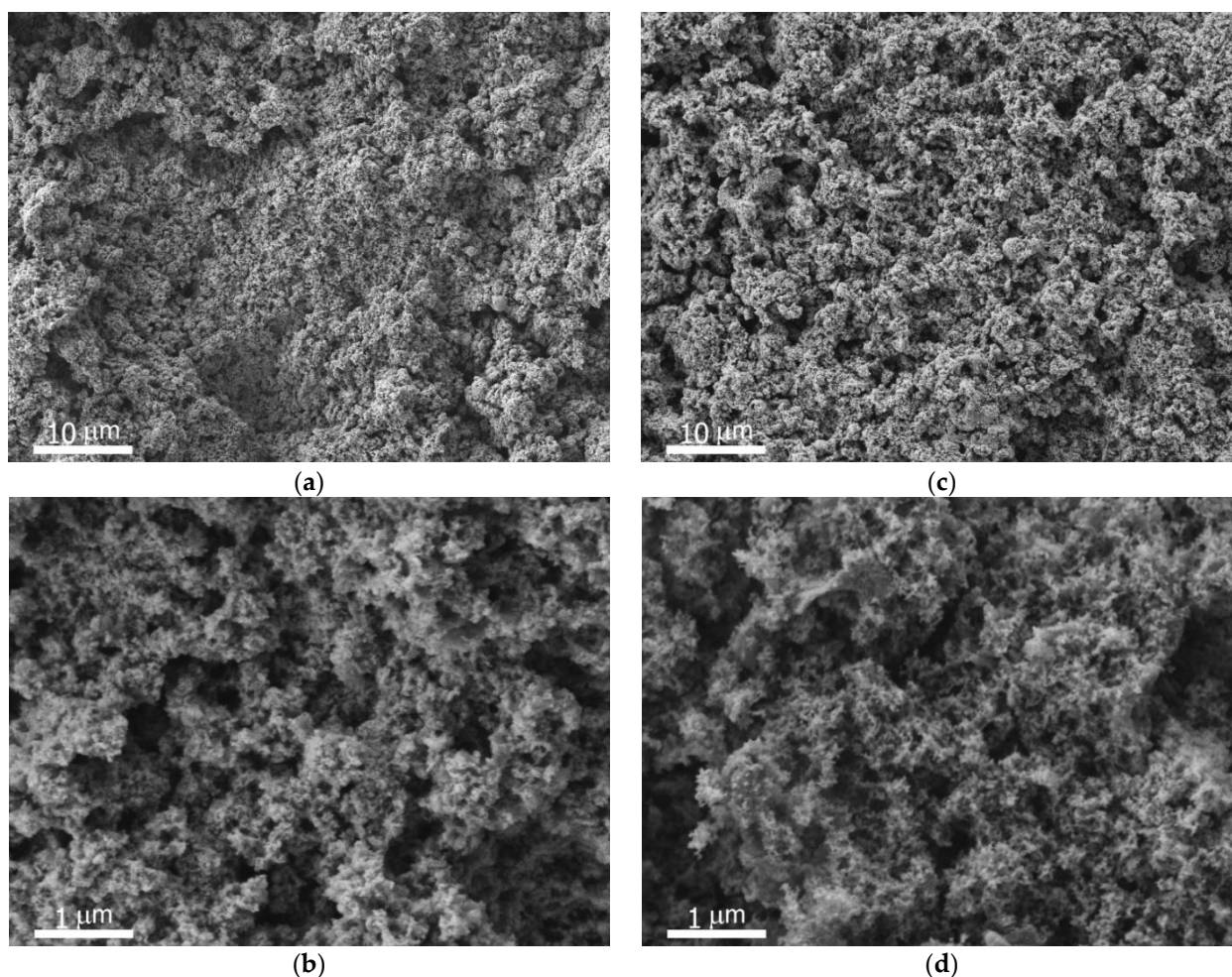


Figure 1. Typical SEM images of the superhydrophobic surface of MA8 alloy at two different magnifications before (a,b) and after (c,d) contact with 0.5 M NaCl solution.

However, after chemisorption of the fluorosilane, the as-prepared samples transformed to the superhydrophobic state with a very high contact angle and low roll-off angle (Table 2).

Table 2. The wettability parameters of the superhydrophobic magnesium sample before and after 30 days of electrochemical tests under continuous contact of the sample with 0.5 M aqueous solutions of NaCl.

Sample	Contact Angle, °	Roll-Off Angle, °
As prepared	171.5 ± 0.7	2.6 ± 0.7
After 30 d of electrochemical tests	168.2 ± 0.5	13.9 ± 4.4

The repetitive measurements of polarization curves and impedance spectra on the same sample, continuously fixed inside the electrochemical cell in contact with 0.5 M sodium chloride solution, causes a weak degradation of the sample. As seen from Table 2, after 30 days of contact with the corrosive liquid and periodic polarization of the sample surface, the sample preserved the superhydrophobic state. The values of contact and roll-off angles of the samples withdrawn from chloride solution, rinsed with water and dried in an oven for 1 h at $T = 150\text{ }^{\circ}\text{C}$ are given in Table 2. These data indicate good chemical resistance of the superhydrophobic layer to the surface polarization and continuous contact with an aqueous solution. To study this point in more detail, we monitored the variation of the water droplet contact angle and roll-off angle in continuous contact with 0.5 M NaCl for 36 days. After 14 and 36 days, the samples were withdrawn from the solution, rinsed in water, and heat-treated in an oven at $T = 150\text{ }^{\circ}\text{C}$ for 1 h. The idea behind washing

and drying was the following: contact with brine or salt spray may lead to adsorption of individual salt crystals to the surface. Even if those crystals didn't cause corrosion (e.g., in the salt spray chamber), they could cover part of the surface, and during measuring of the wettability on unwashed sample instead of measuring the wettability of the coating we would measure the wettability of the salt, which is quite good, but irrelevant. That is why we introduced mild washing with water. The necessity of the subsequent heat treatment was related to weak hydrolysis of the siloxane bonds in fluorooxysilane with formation of the terminal silanol groups, during prolonged contact with brine [29]. The hydrolysis reaction is reversible, and the inverse reaction is promoted at higher temperatures. Thermal treatment of a layer of chemisorbed fluorooxysilane molecules with terminal silanol groups causes the formation of siloxane bonds, leading to the crosslinking of the neighboring chemisorbed molecules. We choose 1 h at 150 °C for unification, as the same temperature and time interval was used during the fabrication of the coating.

To perform the experiments on prolonged contact with brine, two samples were fabricated following a similar protocol. Although the contact and roll-off angles were almost the same for as-prepared samples, the data presented in Figure 2 indicate a slightly different degree of the sample's degradation upon contact with the aggressive liquid. At the same time, the similar features in the behavior of both samples included a sharp increase in water contact angle and a decrease in roll-off angle after 1 h of heat treatment at $T = 150\text{ °C}$ (note that for 14 and 36 days, two measurements (before and after the heat treatment) were displayed in the graphs). Thus, after 36 days of contact with corrosive NaCl solution followed by heat treatment, both samples demonstrated relatively weak deterioration of the contact angle and increase in the roll-off angle compared to the values characteristic of as-prepared samples. The results of the above wettability experiments confirmed the high stability of the chemisorbed layer of the fluorosilane on the textured magnesium alloy surface.

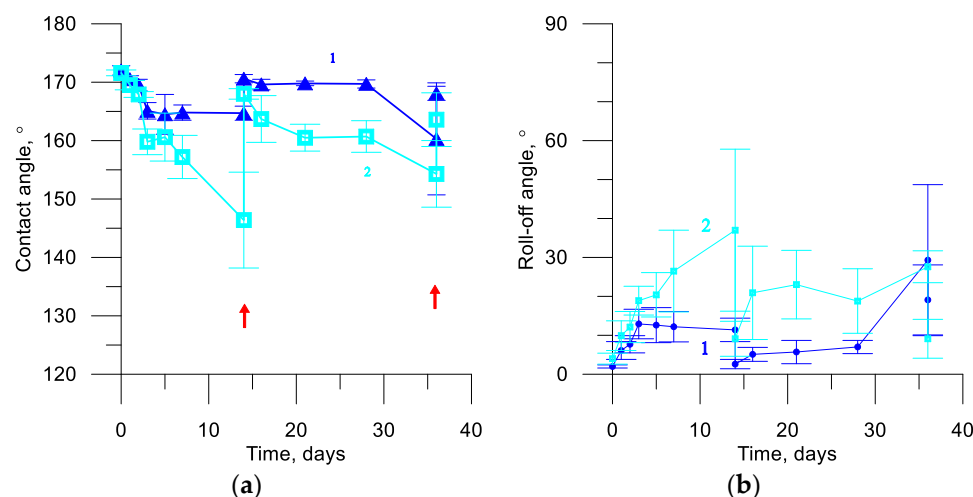


Figure 2. The variation of the water droplet contact angle (a) and roll-off angle (b) for two different superhydrophobic samples (1 and 2) subjected to continuous contact with 0.5 M NaCl for 36 days. The red arrows indicate the times (14 and 36 days) when the samples were washed with values given for both prior and after washing.

3.2. Corrosion Resistance

As it was mentioned in the Section 2.2, the resistance of the fabricated coatings to corrosion processes was studied by the analysis of the evolution of corrosion current and impedance modulus during prolonged immersion of coatings into the 0.5 M aqueous solution of NaCl. Besides, the behavior of the sample in the salt spray chamber was studied. Some of the potentiodynamic polarization curves obtained during continuous contact of the fabricated samples with electrolyte and the evolution of the corrosion current derived

from the polarization curves after Tafel extrapolation are shown in Figure 3a,b, respectively. In the first stage of contact, the corrosion potential somewhat decreased. However, from 6 days of contact to 15 days, a continuous shift of potential of corrosion toward more noble values was detected. Further, the subsequent change in potential ceased.

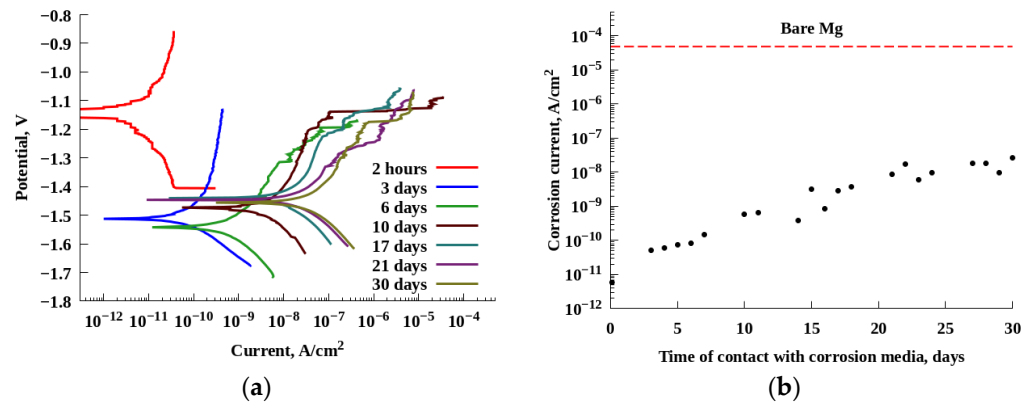


Figure 3. The evolution of potentiodynamic polarization curves (a) and corrosion current density (b) for the superhydrophobic sample subjected to continuous contact with 0.5 M NaCl for 30 days. The dashed line in (b) shows the value of the corrosion current density for the polished MA8 sample after 2 h of contact with the same electrolyte.

The initial value of corrosion current density after 2 h of sample equilibration in the solution was as low as 7×10^{-12} A/cm². This value is more than eight orders of magnitude lower than the characteristic current density for the polished MA8 sample. Subsequent contact with sodium chloride led to gradual and smooth current growth till 8×10^{-8} A/cm² after 30 days of sample immersion into corrosive solution. It is worth noting that the latter value is still four orders of magnitude lower than that obtained for the polished sample which was in contact with electrolyte for 2 h only.

The impedance modulus, which characterizes the barrier property of the surface layer of coating, was simultaneously studied for the same sample during 30 days of contact. The behavior of the impedance modulus spectra (Figure 4) shows to be in line with the behavior of the corrosion current.

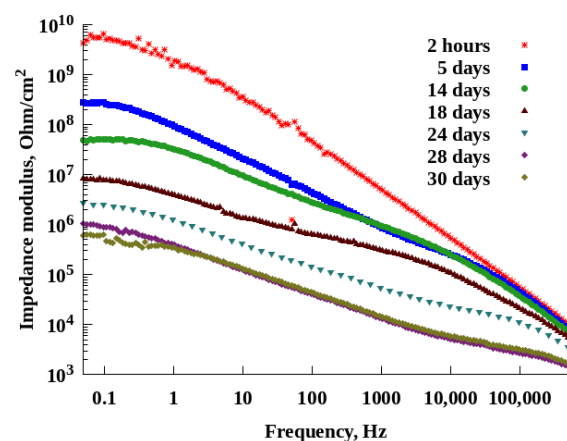


Figure 4. The evolution of the frequency dependence of the electrochemical impedance modulus for the superhydrophobic sample subjected to continuous contact with 0.5 M NaCl for 30 days.

Data presented in Figure 4 indicate continuous deterioration of the impedance modulus $|Z|(\omega)$ for the whole range of studied frequencies. Although the low-frequency modulus $|Z|_{f=0.05}$ decreased during 30 d from 5×10^9 to 6×10^5 Ω /cm² indicating

notable degradation of the barrier properties, the retained barrier properties are still significantly superior to those of the bare alloy. To confirm the high protective potential of the developed coating, we exposed our sample to a salt spray chamber. In this experiment, we compared the protective activity of the developed coating and the hydrophobic coating. Since it was shown earlier [15] that the hydrophobization of bare metal provides a notable degree of corrosion inhibition, the comparison performed here would allow a better understanding of the anticorrosion potential of our superhydrophobic coatings. Before the exposure of the superhydrophobic sample to the salt chamber, the sample was characterized by EIS and by polarization curve measurement. It is worth noting that using the three-electrode electrochemical cell, where the test sample is pressed to the cell wall through the rigid PTFE gasket was accompanied by some deformation of the surface texture of a superhydrophobic sample. The trace of such deformation is typically visualized through the appearance of a white circle on the surface of the sample.

This series of experiments has shown that the first signs of corrosion damage on the surface of polished MA8 sample appeared on the surface already after 15 min of exposure to salt spray; on the hydrophobized surface dark spots appeared after 107 min. An optical image of the hydrophobic (left) and the superhydrophobic samples (right) after 25 h of exposure in the salt spray chamber is shown in Figure 5a. The water contact angle, less than 90° , and the traces of corrosion damage are easily seen on the hydrophobic sample. In contrast, easy roll-off of salt droplets from the surface and absence of damage spots were detected for the superhydrophobic coating. After 250 h of the salt spray test, the surface of the hydrophobic sample was completely covered by the corrosion products, and several deep pittings were formed on top of this coating. For the superhydrophobic coating, the situation was different. The notable area of its surface remained visually intact. Several white patches of magnesium hydroxide of limited area, which mainly occupied the areas of contact between the sample, the PTFE gasket and/or NaCl solution under the electrochemical tests, can be deduced from the image inspection for the sample after 250 h of the salt spray testing. To quantitatively characterize the degradation of both samples in the salt spray chamber, we measured the contact angle formed by the water droplets with the sample's surface. For the initially hydrophobic sample, the droplet spread along the surface with forming a poorly defined asymmetric shape (indicated by the red arrow in the image, Figure 5c) and the contact angle less than 20° . For the superhydrophobic coating, the contact angle varied from the value close to 90° along the circle formed by PTFE gasket, to $140 \pm 10^\circ$ inside the circular zone, and to $154 \pm 5^\circ$ outside the circle. Here we would like to remind that the circular contact between the PTFE gasket and the sample during the preliminary EIS characterization of the sample leads to some deformation of the surface texture, and in some cases can be seen by the naked eye. The behavior of the measured values of the contact angles indicated that although the EIS measurement itself did not cause significant corrosion damage, the nuclei of the hydroxide phase as a product of the corrosion process did appear on the surface during the above experiment.

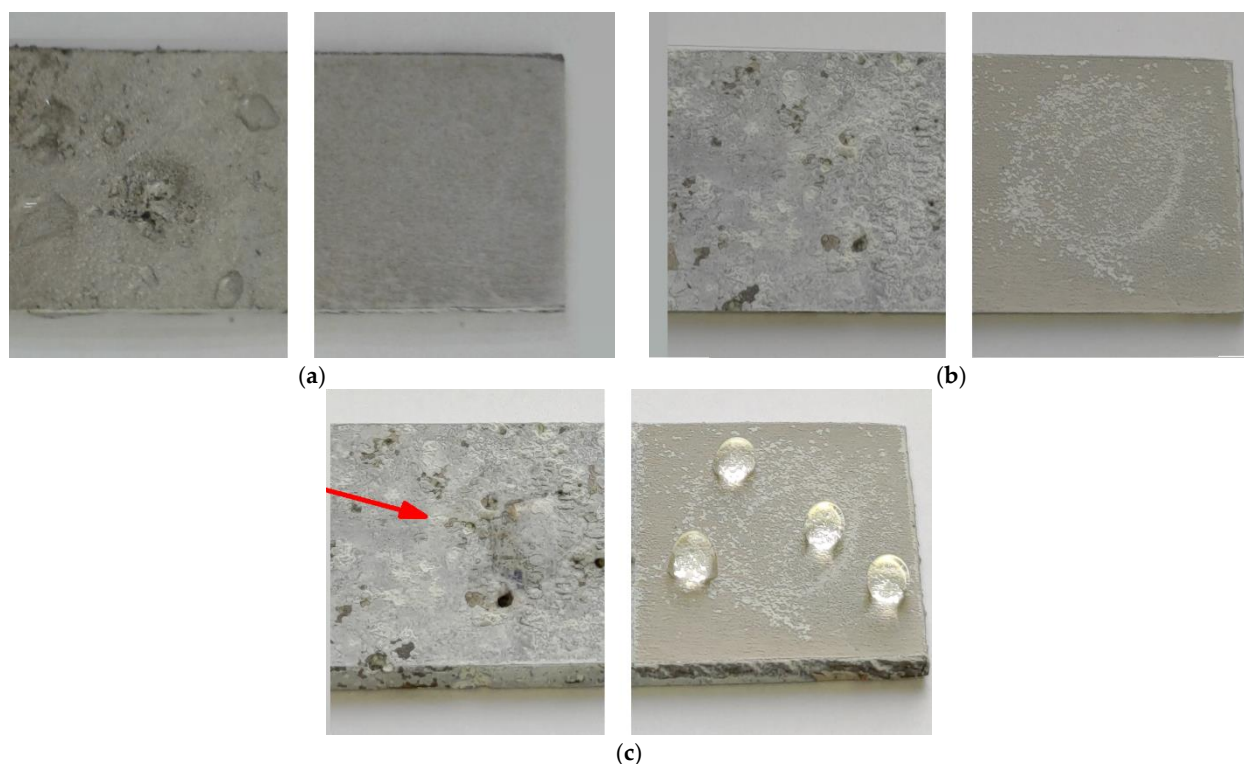


Figure 5. Corrosion of hydrophobic (left) and superhydrophobic (right) samples upon salt fog exposure: (a) after 25 h, (b) after 250 h, (c) after 250 h with subsequent mild washing and drying.

3.3. The Analysis of Protective Mechanisms, Responsible for the Corrosion Resistance of Fabricated Superhydrophobic Coatings on Magnesium Alloy

Data on the prolonged behavior of the fabricated coatings in corrosive environments, presented above, indicated notable resistance of coatings to corrosion damage. The main characteristic feature of these coatings is the superhydrophobic state of their surface. Earlier, the possible mechanisms of corrosion protection by the superhydrophobic coatings on metals were thoroughly discussed in our studies [30,31]. Among the most important mechanisms, the following four should be mentioned:

1. The formation of surface texture with good barrier properties during the process of imparting a hierarchical roughness to the surface;
2. The minimization of the liquid/solid interaction due to the decrease in the area of real contact between the corrosive liquid and the solid, which is a consequence of the water-repelling properties of coating;
3. Chemisorption of the fluorosilane molecules onto the surface-active centers used to decrease the surface energy simultaneously blocks these sites and suppress the adsorption of the corrosive ions onto the surface. Note that such adsorption of corrosive-active ions on the surface is considered as one of the necessary stages of a corrosion process;
4. Surface charging and the formation of a double electric layer. Such charging contributes to the depletion of a surface layer of liquid with corrosive ions, thus leading to a decrease in the corrosiveness of a liquid layer adjacent to the surface.

Now let us consider which of the above mechanisms used to be responsible for the anticorrosion activity of coatings fabricated in this study.

We will begin with the analysis of the barrier properties of the textured layer. Surface heating during laser processing and ablation leads to magnesium oxidation. Thus, it was expected that the main chemical components of the surface layer after laser texturing and hydrophobization are magnesium, magnesium oxide, and fluorosilane. Indeed, this expectation shows to be in agreement with the data of energy dispersion spectroscopy

(Figure 6a), IR spectroscopy (Figure 6b), and XRD (Figure 6c) for the as-prepared sample. From the above data, we can conclude that the surface texture is mainly constituted by magnesium oxide, which has Pilling–Bedworth ratio of less than 0.8 and thus, is porous (see Figure 1a). So, such a layer does not hinder access of corrosion media to bare magnesium which can interact with water with the formation of hydroxide. IR-spectroscopy data, presented by the reflectance spectrum (Figure 6b), also indicate the presence of absorption bands in the range 3620–3470 and 2960–2820 cm^{-1} (shown by red arrows). The former can be attributed to the stretching O-H vibrations in silanol groups formed as a result of the interaction of O-CH₃ terminal groups of the fluorosilane molecule with water molecules. Besides, stretching vibrations in water molecules that form the hydration shells around silanol groups, show the IR activity in the range of 3550–3470 cm^{-1} [32]. The vibrations in the spectral range of 2960–2820 cm^{-1} are associated with the C-H stretching vibrations [31] in the fluorosilane molecule.

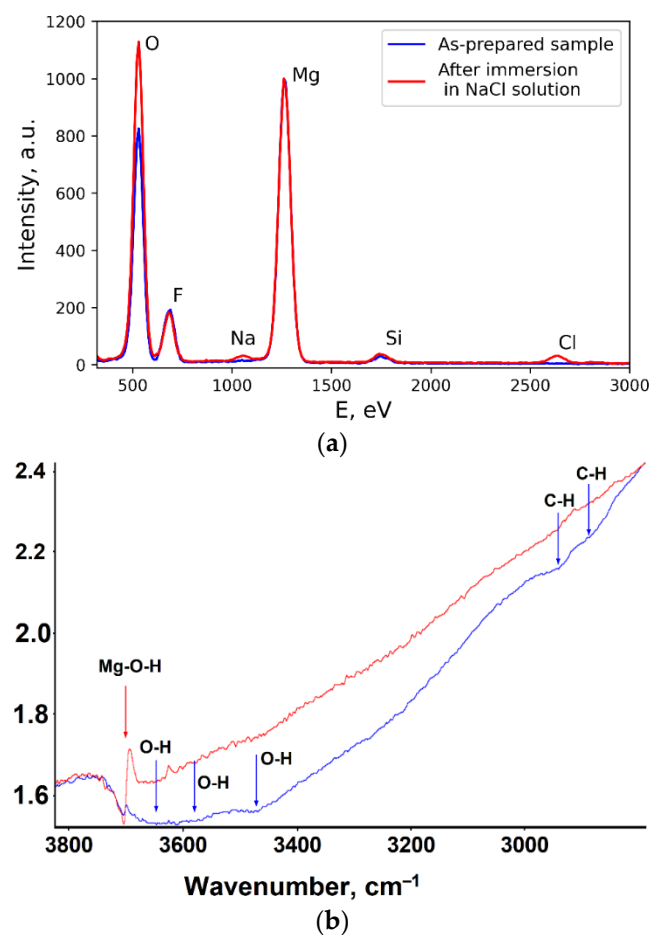


Figure 6. Cont.

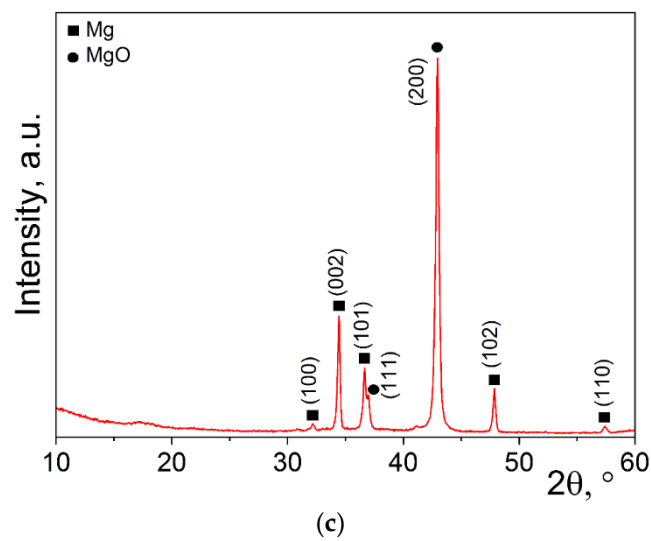


Figure 6. Characterization of the composition of the surface layer for the superhydrophobic coating: (a) EDS spectrum; (b) Fourier-transform infrared reflectance spectra; (c) XRD spectrum. Blue lines in (a,b) correspond to the as-prepared sample, red lines to the sample after immersion in 0.5 M NaCl solution for 30 d; XRD spectra (c) were the same for the samples before and after the immersion.

However, after 30 days of contact of the superhydrophobic sample with corrosive brine, the surface composition somewhat changed. The first evidence for this conclusion comes from the data of scanning electron spectroscopy. A thorough inspection of the surface after prolonged immersion in NaCl solution allowed finding the patches of a new phase (Figure 7), which we assigned as magnesium hydroxide.

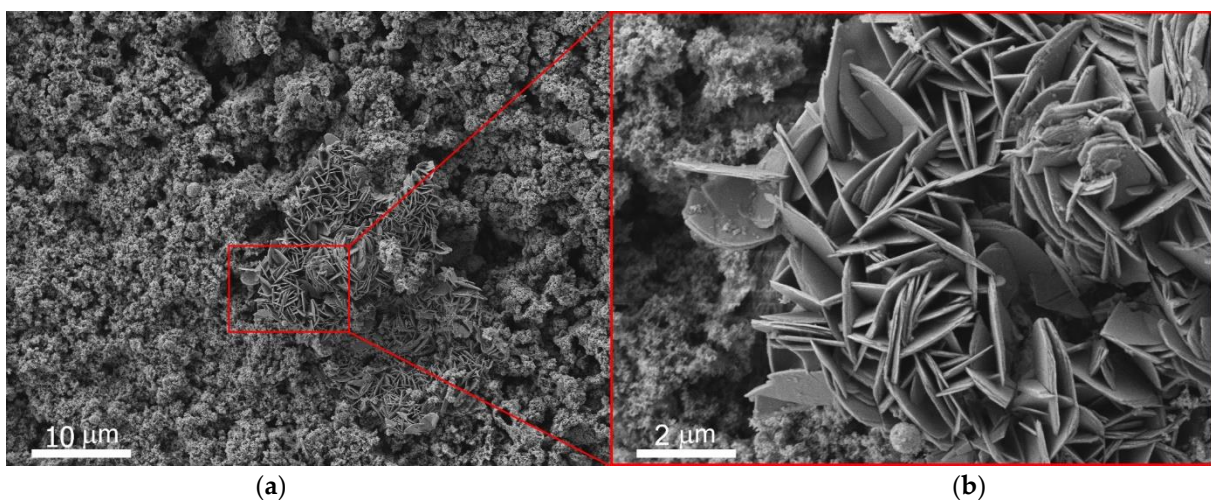


Figure 7. SEM images of the superhydrophobic surface after prolonged immersion in NaCl solution showing the formation of the magnesium hydroxide platelets: (a) survey image; (b) detailed image of the platelets.

For confirmation of this hypothesis, we compared the EDS, XRD, and IR spectroscopy data for the coatings before and after 30 days of immersion.

The grazing reflectance FTIR spectra (Figure 6b), which are sensitive to the variation of the very top surface layer, indicate the appearance of the band $\sim 3700\text{ cm}^{-1}$, which is attributed to O-H stretching vibration in hydroxides [5,32]. The XRD patterns (Figure 6c) indicated the same phase composition for the coating before and after immersion, which can be explained by the weak sensitivity of the method for the variation of the very top monolayers composition. The analysis of energy-dispersive spectra (Figure 6a) before and

after immersion in salt solution led to the conclusion of an increase in the oxygen content, which well agrees with the appearance of traces of the surface hydroxide in IR spectra and SEM images (Figure 7). Besides, the peaks of sodium and chloride in EDS can be considered as an indication of the partial penetration of components of solution inside the texture. At the same time, the small amount of newly formed magnesium hydroxide and the low intensity of Na and Cl peaks convincingly point out the significant impact of the water-repelling properties of the superhydrophobic coatings to the suppression of magnesium dissolution in the corrosive medium, the preservation of the heterogeneous wetting regime, and hindering of the solution imbibition into the coating.

Now let us consider the impact of superhydrophobic surface charging in sodium chloride solution. The sign of the surface charge acquired by the surface in contact with the electrolyte is dependent on the chemical composition of the electrolyte, composition of the very top surface monolayer, and the pH of a solution. Generally, the chemical properties of the surface monolayer of a superhydrophobic coating are determined by the structure and composition of the deposited hydrophobic agent. Careful studies of the solid surface with adsorbed fluorosilane in chloride solutions had shown that in a neutral and alkaline environment the surface is negatively charged [33]. The value of zeta-potential is the higher the lower is the concentration of ions. Thus, according to this study, the surface charge of a superhydrophobic magnesium surface will be negative and will repulse the aggressive chloride anions from the surface. The latter promotes the stronger corrosion resistance of the coatings, the lower is the bulk concentration of ions. This point is significant for explaining the more rapid degradation of fabricated coatings in salt spray chamber compared to continuous contact with the corrosive solution in electrochemical tests. Since in the chamber the sprayed brine droplets deposited onto the surface evaporated due to elevated temperature inside the chamber, the salt could accumulate on the surface. Hence, the concentration of droplets of the electrolyte continuously grew in the course of sample exposure. The latter resulted in the decrease in surface zeta-potential, weakening of chloride ions repulsion from the surface, and increase in the concentration of these ions in the close proximity of the metal surface, thus increasing the probability of ion adsorption to it.

Finally, let us discuss the role of an adsorbed layer of fluorosilane in the suppression of chloride ions adsorption on the coating as a stage of the corrosion process. The efficiency of this mechanism for our system is clearly demonstrated by the inhibition of the corrosion process on the hydrophobic sample compared to the polished one in conditions of the salt spray chamber. As discussed in Section 3.2, the time required for the appearance of the first signs of corrosion damage on the polished MA8 was seven times lower than that for the hydrophobized MA8. However, the main difference between these two surfaces in conditions of periodic deposition of concentrated salt droplets and their drying with the formation of salt deposits was related to the occupation of surface sites, available for chloride ions adsorption, by the molecules of fluorosilanes.

Thus, the analysis performed above, clearly shows that among four mechanisms generally responsible for the corrosion protection by the superhydrophobic coatings, only the mechanism related to the enhanced barrier properties of the surface texture was ineffective for our coating, while the three others provided prolonged chemical and corrosion stability in the corrosive medium.

4. Conclusions

Here we described the technologically simple route of fabrication of the superhydrophobic coating on top of wrought magnesium alloy MA8 based on nanosecond laser processing followed by the chemical vapor deposition of fluorosilane. We have shown that for this alloy, which is intrinsically characterized by very poor corrosion resistance, the corrosion protection in continuous contact with sodium chloride solution or in periodic contact with a salt spray can be achieved by the deposition of the chemically stable superhydrophobic coating. The behavior of the surface and electrochemical parameters

of the fabricated coating during its prolonged and continuous contact with the corrosive medium was studied by the combination of physicochemical methods. It was shown that such coatings are appropriate for the protection of magnesium alloy surfaces in corrosive environments for many days.

Despite the simple route of preparation of coatings reported here, their efficiency shows to be comparable with the best discussed in the literature coatings having complex structure and composition [12,13]. Since the reliability of the anticorrosion systems is critically dependent on their complexity, the coatings fabricated in this study look very attractive for practical applications.

Author Contributions: Conceptualization, A.M.E., K.A.E. and L.B.B.; methodology, K.A.E. and A.M.E.; investigation, A.M.S., V.V.P., K.A.E., A.G.D. and E.V.C.; writing—original draft preparation, L.B.B.; writing—review and editing, A.M.E. and L.B.B.; visualization, A.M.E., K.A.E. and A.G.D.; supervision, L.B.B.; project administration, A.M.E.; funding acquisition, A.M.E. and K.A.E. All authors have read and agreed to the published version of the manuscript.

Funding: This research was partially funded by the Russian Foundation for Basic Research (grant #20-53-56066). The selection of regimes for sample fabrication was conducted under the Russian Federation President's grant for young research groups MK-2124.2021.1.3.

Institutional Review Board Statement: Not applicable.

Informed Consent Statement: Not applicable.

Data Availability Statement: Data are contained within the article.

Acknowledgments: The SEM and EDX studies were performed using the equipment of the IGIC RAS Joint Research Centre for Physical Methods of Research.

Conflicts of Interest: The authors declare no conflict of interest. The funders had no role in the design of the study; in the collection, analyses, or interpretation of data; in the writing of the manuscript, or in the decision to publish the results.

References

1. Esmaily, M.; Svensson, J.E.; Fajardo, S.; Birbilis, N.; Frankel, G.S.; Virtanen, S.; Arrabal, R.; Thomas, S.; Johansson, L.G. Fundamentals and advances in magnesium alloy corrosion. *Prog. Mater. Sci.* **2017**, *89*, 92–193. [[CrossRef](#)]
2. Montemor, M.F. Functional and smart coatings for corrosion protection: A review of recent advances. *Surf. Coat. Technol.* **2014**, *258*, 17–37. [[CrossRef](#)]
3. Zhang, D.D.; Peng, F.; Liu, X.Y. Protection of magnesium alloys: From physical barrier coating to smart self-healing coating. *J. Alloy. Compd.* **2021**, *853*, 157010. [[CrossRef](#)]
4. Larson, C.; Smith, J.R.; Armstrong, G.J. Current research on surface finishing and coatings for aerospace bodies and structures—A review. *Trans. Inst. Met. Finish.* **2013**, *91*, 120–132. [[CrossRef](#)]
5. Barranco, V.; Carmona, N.; Galvan, J.C.; Grobelny, M.; Kwiatkowski, L.; Villegas, M.A. Electrochemical study of tailored sol-gel thin films as pre-treatment prior to organic coating for AZ91 magnesium alloy. *Prog. Org. Coat.* **2010**, *68*, 347–355. [[CrossRef](#)]
6. Lkhagvaa, T.; Rehman, Z.U.; Choi, D. Post-anodization methods for improved anticorrosion properties: A review. *J. Coat. Technol. Res.* **2021**, *18*, 1–17. [[CrossRef](#)]
7. DeForce, B.S.; Eden, T.J.; Potter, J.K. Cold spray Al-5% Mg coatings for the corrosion protection of magnesium alloys. *J. Therm. Spray Technol.* **2011**, *20*, 1352–1358. [[CrossRef](#)]
8. Zhang, X.F.; Zhang, M.; Li, R.H.; Feng, X.Y.; Pang, X.; Rao, J.S.; Cong, D.L.; Yin, C.Q.; Zhang, Y.X. Active corrosion protection of Mg-Al layered double hydroxide for magnesium alloys: A short review. *Coatings* **2021**, *11*, 1316. [[CrossRef](#)]
9. Ishizaki, T.; Chiba, S.; Watanabe, K.; Suzuki, H. Corrosion resistance of Mg-Al layered double hydroxide container-containing magnesium hydroxide films formed directly on magnesium alloy by chemical-free steam coating. *J. Mater. Chem. A* **2013**, *1*, 8968–8977. [[CrossRef](#)]
10. Phuong, N.V.; Gupta, M.; Moon, S. Enhanced corrosion performance of magnesium phosphate conversion coating on AZ31 magnesium alloy. *Trans. Nonferrous Met. Soc. China* **2017**, *27*, 1087–1095. [[CrossRef](#)]
11. Ishizaki, T.; Shigematsu, I.; Saito, N. Anticorrosive magnesium phosphate coating on AZ31 magnesium alloy. *Surf. Coat. Technol.* **2009**, *203*, 2288–2291. [[CrossRef](#)]
12. Wang, Y.; Zhou, X.; Yin, M.; Pu, J.; Yuan, N.; Ding, J. Superhydrophobic and self-healing Mg-Al layered double hydroxide/silane composite coatings on the Mg alloy surface with a long-term anti-corrosion lifetime. *Langmuir* **2021**, *37*, 8129–8138. [[CrossRef](#)] [[PubMed](#)]

13. Zhang, J.; Wei, J.; Li, B.; Zhao, X.; Zhang, J. Long-term corrosion protection for magnesium alloy by two-layer self-healing superamphiphobic coatings based on shape memory polymers and attapulgite. *J. Colloid Interface Sci.* **2021**, *594*, 836–847. [[CrossRef](#)] [[PubMed](#)]
14. Al Zoubi, W.; Kim, M.J.; Kim, Y.G.; Ko, Y.G. Fabrication of graphene oxide/8-hydroxyquinolin/inorganic coating on the magnesium surface for extraordinary corrosion protection. *Prog. Org. Coat.* **2019**, *137*, 105314. [[CrossRef](#)]
15. Boinovich, L.B.; Emelyanenko, A.M.; Pashinin, A.S.; Gnedenkov, S.V.; Egorin, V.S.; Sinebryukhov, S.L. Mg alloy treatment for superhydrophobic anticorrosion coatings formation. *Surf. Innov.* **2013**, *1*, 162–172. [[CrossRef](#)]
16. Yang, Z.; Liu, X.P.; Tian, Y.L. A contrastive investigation on anticorrosive performance of laser-induced super-hydrophobic and oil-infused slippery coatings. *Prog. Org. Coat.* **2020**, *138*, 105313. [[CrossRef](#)]
17. Safarpour, M.; Hosseini, S.A.; Ahadani-Targhi, F.; Vasina, P.; Alishahi, M. A transition from petal-state to lotus-state in AZ91 magnesium surface by tailoring the microstructure. *Surf. Coat. Technol.* **2020**, *383*, 125239. [[CrossRef](#)]
18. Emelyanenko, A.M.; Kaminsky, V.V.; Pytskii, I.S.; Emelyanenko, K.A.; Domantovsky, A.G.; Chulkova, E.V.; Aleshkin, A.V.; Boinovich, L.B. Antimicrobial activity and degradation of superhydrophobic magnesium substrates in bacterial media. *Metals* **2021**, *11*, 1100. [[CrossRef](#)]
19. Joo, J.; Kim, D.; Moon, H.S.; Kim, K.; Lee, J. Durable anti-corrosive oil-impregnated porous surface of magnesium alloy by plasma electrolytic oxidation with hydrothermal treatment. *Appl. Surf. Sci.* **2020**, *509*, 145361. [[CrossRef](#)]
20. Saji, V.S. Recent progress in superhydrophobic and superamphiphobic coatings for magnesium and its alloys. *J. Magnes. Alloy.* **2021**, *9*, 748–778. [[CrossRef](#)]
21. Emelyanenko, K.A.; Domantovsky, A.G.; Chulkova, E.V.; Emelyanenko, A.M.; Boinovich, L.B. Thermally induced gradient of properties on a superhydrophobic magnesium alloy surface. *Metals* **2021**, *11*, 41. [[CrossRef](#)]
22. Venkatesh, R.; Manivannan, S.; Sakthivel, P.; Vijayan, V.; Jidesh, S. The investigation on newly developed of hydrophobic coating on cast AZ91D magnesium alloy under 3.5 wt% NaCl solutions. *J. Inorg. Organomet. Polym. Mater.* **2021**, *29*, 1–3. [[CrossRef](#)]
23. Yeganeh, M.; Mohammadi, N. Superhydrophobic surface of Mg alloys: A review. *J. Magnes. Alloy.* **2018**, *6*, 59–70. [[CrossRef](#)]
24. Yao, W.; Chen, Y.; Wu, L.; Zhang, J.; Pan, F. Effective corrosion and wear protection of slippery liquid-infused porous surface on AZ31 Mg alloy. *Surf. Coat. Technol.* **2022**, *429*, 127953. [[CrossRef](#)]
25. Emelyanenko, A.M.; Boinovich, L.B. The role of discretization at the video image processing of sessile and pendant drop profiles. *Colloids Surf. A* **2001**, *189*, 197–202. [[CrossRef](#)]
26. Chulkova, E.V.; Emelyanenko, K.A.; Emelyanenko, A.M.; Boinovich, L.B. Elimination of wetting study flaws in unsaturated vapors based on Laplace fit parameters. *Surf. Innov.* **2022**, *10*, 21–24. [[CrossRef](#)]
27. Tan, Q.Y.; Atrens, A.; Mo, N.; Zhang, M.X. Oxidation of magnesium alloys at elevated temperatures in air: A review. *Corros. Sci.* **2016**, *112*, 734–759. [[CrossRef](#)]
28. Pilling, N.B.; Bedworth, R.E. The oxidation of metals at high temperatures. *J. Inst. Met.* **1923**, *29*, 529–591.
29. Boinovich, L.B.; Emelyanenko, A.M. The behaviour of fluoro- and hydrocarbon surfactants used for fabrication of superhydrophobic coatings at solid/water interface. *Colloids Surf. A* **2015**, *481*, 167–175. [[CrossRef](#)]
30. Boinovich, L.B.; Emelyanenko, A.M.; Modestov, A.D.; Domantovsky, A.G.; Shiryaev, A.A.; Emelyanenko, K.A.; Dvoretzkaya, O.V.; Ganne, A.A. Corrosion behavior of superhydrophobic aluminum alloy in concentrated potassium halide solutions: When the specific anion effect is manifested. *Corros. Sci.* **2016**, *112*, 517–527. [[CrossRef](#)]
31. Boinovich, L.B.; Emelyanenko, A.M.; Modestov, A.D.; Domantovsky, A.G.; Emelyanenko, K.A. Not simply repel water: The diversified nature of corrosion protection by superhydrophobic coatings. *Mendeleev Commun.* **2017**, *27*, 254–256. [[CrossRef](#)]
32. Smith, A.L. *Applied Infrared Spectroscopy*; John Wiley: New York, NY, USA, 1979.
33. Boinovich, L.B.; Sobolev, V.D.; Maslakov, K.I.; Domantovsky, A.G.; Sergeeva, I.P.; Emelyanenko, A.M. Cation capture and overcharging of a hydrophobized quartz surface in concentrated potassium chloride solutions. *Colloids Surf. A* **2018**, *537*, 76–84. [[CrossRef](#)]